

RSC Advances



This is an *Accepted Manuscript*, which has been through the Royal Society of Chemistry peer review process and has been accepted for publication.

Accepted Manuscripts are published online shortly after acceptance, before technical editing, formatting and proof reading. Using this free service, authors can make their results available to the community, in citable form, before we publish the edited article. This *Accepted Manuscript* will be replaced by the edited, formatted and paginated article as soon as this is available.

You can find more information about *Accepted Manuscripts* in the [Information for Authors](#).

Please note that technical editing may introduce minor changes to the text and/or graphics, which may alter content. The journal's standard [Terms & Conditions](#) and the [Ethical guidelines](#) still apply. In no event shall the Royal Society of Chemistry be held responsible for any errors or omissions in this *Accepted Manuscript* or any consequences arising from the use of any information it contains.

ARTICLE

Atom Efficient Thermal and Photocuring Combined Treatments for the Synthesis of Novel Eco-Friendly Grid-Like Zein Nanofibres

Cite this: DOI: 10.1039/x0xx00000x

Received 00th January 2012,
Accepted 00th January 2012

DOI: 10.1039/x0xx00000x

www.rsc.org/

Qingqing Wang,^a Avinav G. Nandgaonkar,^{b,c} Jing Cui,^a Fenglin Huang,^a Wendy E. Krause,^c Lucian A. Lucia,^{**b,c,d} Qufu Wei^{*a}

Herein is reported for the first time a novel crosslinking approach for the synthesis of grid-like zein nanofibres with SbQ (styrylpyridinequatarnary) realized by a simple electrospinning process followed by thermal treatment and/or UV illumination. The properties of the electrospinning solution such as viscosity, conductivity, and surface tension were tested to evaluate the effect of SbQ addition (0 wt-%, 10 wt-%, 20 wt-%) on the electrospinnability glacial acetic acid solution of the zein (25 wt-%). The incorporation of SbQ resulted in bead-free nanofibres structures with increased diameter compared to pure zein nanofibres. The FT-IR results indicated that the zein glacial acidic acid protein solution crosslinked, a phenomenon that can be characterized by two discrete, temporally distinct events: inter-molecular solution crosslinking and intra-fiber crosslinking from the SbQ throughout the nanofibrous mat following photocuring. The SbQ can form intra-fiber bridges as confirmed by the SEM images; on a macroscopic (gross) scale, the crosslinking manifests itself by the formation of grid-like structures. The thermal properties of the zein nanofibres, however, were minimally improved after the incorporation of SbQ although the cured composite nanofibres demonstrated significantly improved tensile and elongation properties.

Introduction

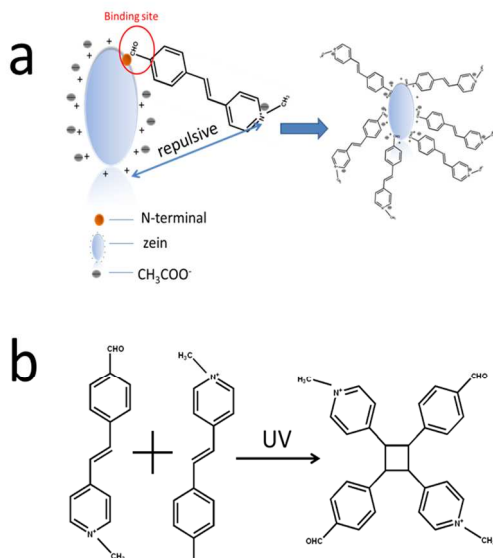
Electrospinning (ES) is a fundamentally appealing, simple, and versatile technique to produce extremely fine fibrous structures with diameters ranging from 100 nanometres to several micrometres. The topic of electrospinning fibers has received significant attention over the last decade because of the nanoscopic dimension, large surface area-to-volume ratio, and small pore size of the resultant fibres relative to their macroscopic counterparts.¹ Not surprisingly, biocompatible electrospun nanofibrous materials have found wide acceptance in the biomedical arena within fields as diverse as tissue engineering scaffolding,² drug delivery,³ wound dressing,⁴ and protective clothing.⁵

One of the more universally appealing biocompatible materials that has garnered significant attention recently is zein. Zein, a protein from corn, is available as a by-product of starch processing.⁶ Zein has received considerable attention due to its non-toxic, biocompatible, biodegradable nature as well as its excellent film-forming capabilities.⁷ These latter unique film-forming properties of electrospun zein nanofibres provide a number of applications; for example, they can be used in the encapsulation of essential oils, as antioxidants, aromas and flavors in functional food packaging materials,⁸⁻¹⁰ wound dressings,¹¹ and scaffolding materials for cell/tissue cultures.¹²

However, the poor mechanical properties of zein have drastically restricted any further applications, especially those involving mechanical tolerances; this adversity has usually been addressed by using plasticizers or crosslinking reagents. However, plasticizers such as triethylene glycol have negatively affected the mechanical properties of zein films by contributing to unacceptably enhanced elongation rates without concomitant high strengths and Young's moduli.¹³ An alternative approach to addressing its inherent mechanical handicap is to invoke crosslinking agents. Several of the most frequently invoked crosslinking agents are formaldehyde,¹⁴ glyoxal,¹⁵ and glutaraldehyde (GDA).¹⁶⁻¹⁸ Unfortunately, these crosslinking agents are not as green as desired, while their products suffer from significantly diminished elongation properties. Other relatively green crosslinking reagents have been reported, such as hexamethylenediisocyanate (HDI),¹⁹ polycarboxylic acids,²⁰ carbodiimide,²² to name a few. Yet, the final products still suffer from either a lack of either one or a combination of mechanical properties or environmental friendliness. Herein, a novel atom efficient and two-step crosslinking process is proposed to overcome the inherent lack of desirable physical properties of zein fibrous materials.

SbQ, an amphiphilic sensitizer of the styrylpyridinium family, can be dimerised via an atom economic [2+2] orbitally-conserved cyclo addition reaction triggered by UV radiation

(Scheme 1b).²³ SbQ is typically reported along with poly(vinyl alcohol) (PVA) as a covalently grafted pendant group on a polymer backbone.²⁴ In a recent report, the self-assembly (complexation) behavior of SbQ with oppositely charged polyelectrolytes in aqueous solution is an additional coupling technique that was successfully studied as a model system for transporting pharmacologically relevant materials such as paclitaxel (PTX), a mitotic inhibitory agent used extensively as a cancer therapeutic.²⁵ The ability to direct complexed SbQ as a delivery agent for a PTX load demonstrated a promising avenue for delivering *hydrophobic* chemotherapeutic drugs to tumors.²⁵ However, to date, there is no evidence of studies that have focused on the crosslinking ability of SbQ as a means to selectively couple it to proteins such as zein.



Scheme 1. (a) self-assembly behavior between zein and SbQ in AcOH solution and (b) a generic highly atom efficient and conserved photo-dimerization (UV radiation-driven) equation for SbQ.

Therefore, this work reports for the first time the electrospinning of SbQ from a zein/glacial acetic acid (AcOH) solution into zein/SbQ composite nanofibers that is immediately followed by thermal treatment and UV illumination to induce crosslinking between SbQ and zein. Serendipitously, an incipient self-assembly behavior between zein and SbQ in AcOH solution occurs to further enhance the final chemistry and is illustrated in Scheme 1a, while the photochemistry of SbQ is illustrated in Scheme 1b. The morphological, structural, thermal, and mechanical properties of the resulting electrospun zein nanofibers were analyzed before and after crosslinking by SEM, FT-IR, TGA, DSC, and a tensile tester.

Results and discussion

The influence of loaded SbQ on the properties of electrospun solutions

Table 1. Viscosity, conductivity, surface tension, and average as-spun fiber diameter of SbQ-loaded zein solutions.

Samples	Viscosity (mPa·s)	Conductivity ($\mu\text{S cm}^{-1}$)	Surface tension (mNm ⁻¹)	Average diameter (nm)
Zein	295±7.1	92.0±1.9	33.1±1.1	261.4±98.6
Zein90/SbQ10	417.5±3.5	64.6±2.3	33.0±0.3	395.3±89.6
Zein80/SbQ20	495±7.1	19.4±0.8	32.4±0.7	451.4±89.7

Zein	295±7.1	92.0±1.9	33.1±1.1	261.4±98.6
Zein90/SbQ10	417.5±3.5	64.6±2.3	33.0±0.3	395.3±89.6
Zein80/SbQ20	495±7.1	19.4±0.8	32.4±0.7	451.4±89.7

A number of properties for the electrospinning solutions at varying levels of SbQ were measured and are shown in Table 1. The addition of SbQ into the zein/HAc solutions clearly increased the viscosity of the solutions (295 → 495 mPa·s), while the solution conductivity markedly dropped with increasing SbQ, from $92\mu\text{S cm}^{-1}$ for pure zein/AcOH solution to $64\mu\text{S cm}^{-1}$ and $19\mu\text{S cm}^{-1}$ for Zein90/SbQ10/AcOH and Zein80/SbQ20/AcOH solutions, respectively. Additionally, the surface tension did not significantly change with the addition of SbQ. The increase in viscosity and decrease in conductivity were two significant factors that contributed to a great extent to the gradual increase in fibre diameter.

The morphology of the as-spun zein and zein/SbQ nanofibers with different levels of SbQ

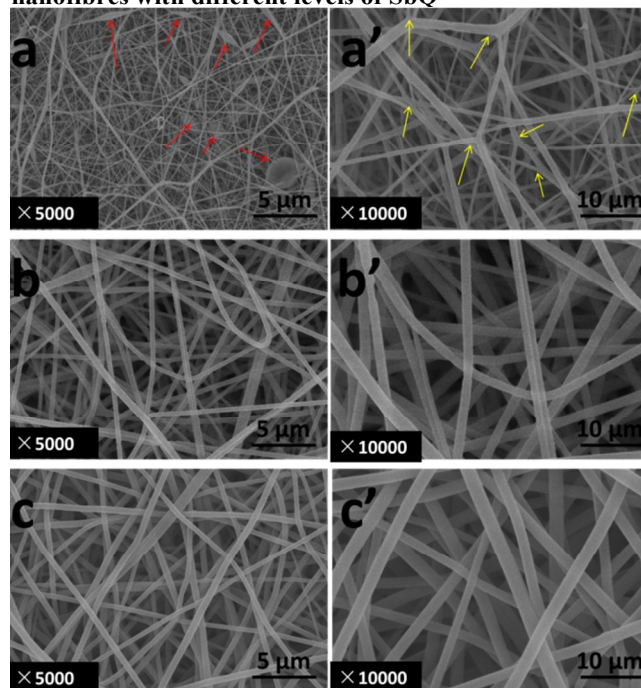


Fig. 1 SEM microphotographs of (a&a') zein (25 wt-%), (b&b') zein90/SbQ10, (c&c') zein80/SbQ20.

Representative SEM images of the electrospun nanofibers are shown in Fig.1. The pure zein nanofibers demonstrated a beaded structure (Fig.1 a), whereas in a more magnified image, the branched structure can also be seen (Fig. 1 a'). After the addition of SbQ, the electrospinnability of zein solutions improved and bead-free individual nanofibers were obtained (Fig.1 b&b', c&c'). Also, it was discovered that the average fibre diameter increased upon the addition of SbQ. The average diameters for the SbQ loaded fibres increased from 261 nm to 395 nm and 451 nm for zein90/SbQ10 and zein80/SbQ20, respectively. The SbQ content increased the viscosity of the solutions due to increased molecular entanglements in the solution. With respect to conductivity, the addition of SbQ decreased the solution conductivity because of an electrostatic adsorption effect between SbQ and ionized

AcOH as shown in Scheme 1a. Thus, it can be inferred that addition of SbQ resulted in increased fibre diameter due to a more compact (less “stretched”) electrified Taylor Cone plume.²⁶

The morphology of the zein/SbQ composite nanofibres after thermal or photocuring

Pristine zein nanofibrous membranes are easily shrunk in water and have poor mechanical strength. Therefore, the crosslinking of zein nanofibres is a necessary protocol for any attendant mechanical gains. For the crosslinking treatment, zein80/SbQ20 was selected as the prototypical sample because it displayed the best fibre morphology.

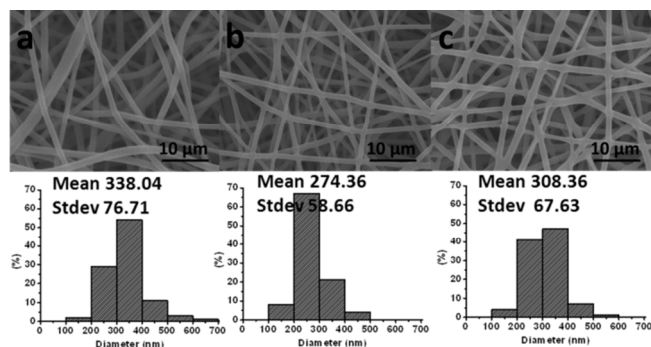


Fig. 2 SEM images of zein80/SbQ20 after different post treatment methods: (a) thermal treatment; (b) UV illumination; (c) thermal treatment + UV illumination.

After different post-treatment processes, the zein/SbQ composite nanofibres showed distinct morphologies (Fig. 2). After the thermal treatment, the composite nanofibres showed a very similar structure as that of zein/SbQ nanofibres, only differing in their relatively smaller diameter of 338 nm compared to the original 451 nm (Fig.2 a). However, after UV illumination, the average diameter of the fibres significantly decreased to ~ 274 nm, evidence to the incidence of photo-crosslinking within the fibrous network (Fig.2 b). The diameter of the final zein/SbQ composite nanofibres obtained from a combined thermal and UV illumination treatment was not surprisingly different between that of the other two samples; it may be thus inferred that the thermal treatment may contribute to a more stable structure that resists diameter shrinkage under UV-induced crosslinking (Fig.2 c). Also, the fibre morphology changed from cylindrical to fused after the combined treatment. Similar results have also been reported when zein/chitosan/PVP electrospun fibres were crosslinked in a tetrahydrofuran (THF) solution containing 1 wt-% HDI.²⁷

Interaction between zein and SbQ

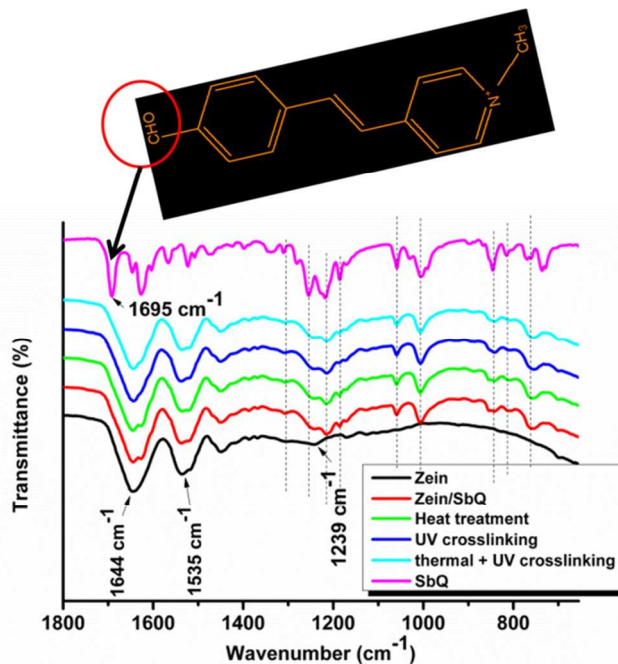


Fig. 3 FT-IR spectra of zein, zein/SbQ before and after thermal and photocuring.

The ATR-FT-IR spectra over 650-1800 cm⁻¹ are shown in Fig. 3. The zein/SbQ composite nanofibrous membrane containing 20 wt-% SbQ was again chosen as the representative sample because of its morphology. Pure zein nanofibres have three characteristic vibrational bands: amide 1 (1644 cm⁻¹), amide 2 (1535 cm⁻¹) and amide 3 (1239 cm⁻¹), which correspond to C=O stretching, C-N stretching, and N-H in-plane deformation, respectively.¹⁷ Upon addition of SbQ, the secondary structure of zein changed, while most of the chemical groups of SbQ were well maintained and clearly present in the spectra of zein/SbQ, except that the band at 1695 cm⁻¹ (-CHO group of SbQ) completely disappeared.

As previously alluded, one of the predominant reaction products of protein -CHO groups with reagents such as glutaraldehyde (GDA), glyoxal, and formaldehyde is a conjugative Schiff base (e.g., a condensation with an ε-amino group of lysine).²⁸ However, in this case, zein lacks lysine, but instead possesses three sulfhydryl groups;²⁹ the only other nucleophilic functional groups that may be available for reaction with the SbQ -CHO group are the N-terminal α-NH₂ groups, the imidazole ring of histidine, and the phenolic group of tyrosine.³⁰ Fortunately in this case, in addition to ethanol and acetone, acetic acid has been reported to have catalytic properties for protein crosslinking.¹⁷

After a period of reaction in acetic acid, the -CHO group of SbQ disappeared and the amide 3 absorption band of zein shifted from 1239 cm⁻¹ to 1247 cm⁻¹, indicative of a chemical reaction between SbQ and zein.

Thermal behaviour of zein/SbQ composite nanofibres

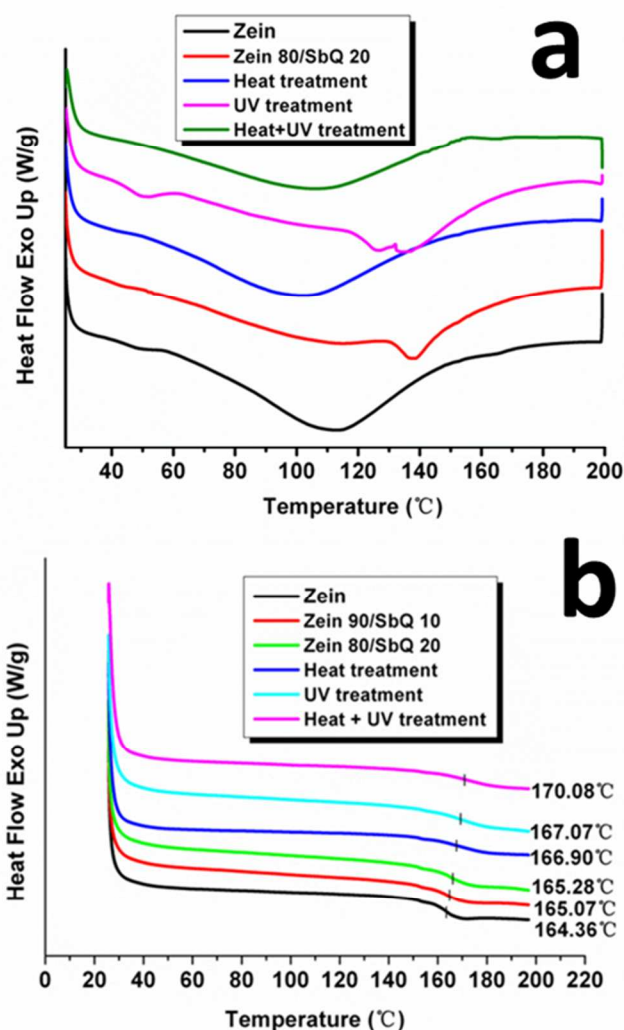


Fig. 4 DSC thermograms of zein/SbQ composite nanofibres (a) first scan, (b) second scan.

The DSC thermograms of the control and zein/SbQ composite nanofibres following different post-treatments are shown in Fig. 4. From the first scan of the DSC thermograms (Fig. 4 a), it is seen that different post-treatments lead to very different thermal behaviours. For pure zein fabric, a broad endothermic peak having a peak maximum at ~ 117 °C, exactly the boiling point of acetic acid. After the addition of SbQ, a sharp peak at ~ 140 °C was seen that may be attributed to ionized acetic acid bound by positively charged SbQ. An electrostatic effect would easily make bound acetic acid more difficult to evaporate, so hence the higher temperature. After thermal treatment (120 °C, 2 hours), the acetic acid disappeared. The peak maximum shifted to ~ 100 °C indicating that the samples contained water.

The second scan of the DSC thermograms (Fig. 4 b) clearly showed the glass transition temperature (T_g) of all samples. The addition of SbQ did not have a significant effect on augmenting the T_g value, but UV illumination, especially when combined with thermal treatment, improved the T_g from 164 °C to 167 °C and to 170 °C in conjunction with thermal treatment. An increase in T_g is likely due to restricted chain mobility in zein because of the photo-crosslinked SbQ moieties.

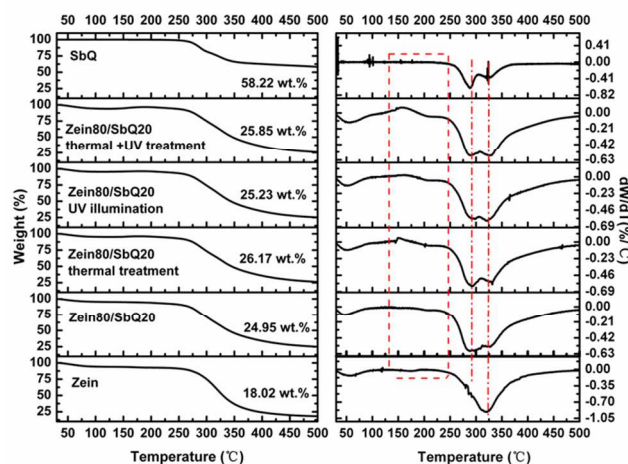


Fig. 5 TGA and DTGA thermograms of SbQ, Zein nanofibers, Zein/SbQ composite nanofibers before and after post treatment; the residual weight ratio at 500 °C is presented in the graph.

TGA was used to evaluate and compare the thermal stabilities of the zein/SbQ composite nanofibres after different post-treatments. As shown in Fig. 5, zein and zein/SbQ composite nanofibres with different post-treatments showed a mass loss from 50 to 250 °C, which may be attributed to acetic acid or water entrapped within the film matrix. The thermogram of SbQ showed two stages of degradation: the second stage was in the same temperature regime as that of zein. From the thermograms of all these samples, it can be concluded that the incorporation of SbQ did not appreciably change the thermal stability of the zein nanofibres.

Water absorption behaviour of zein/SbQ composite nanofibres

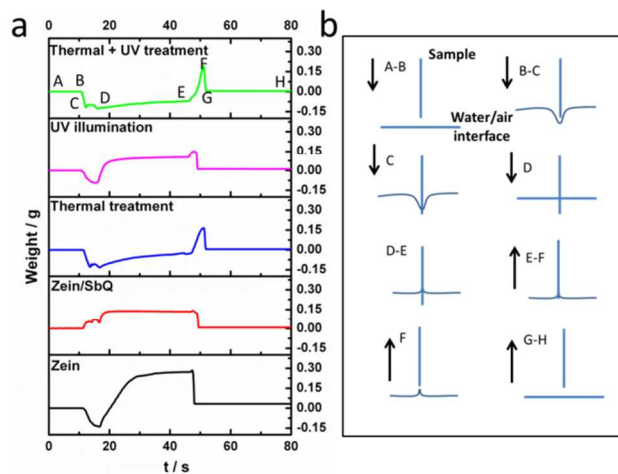


Fig. 6 (a) Water absorption behaviour of zein, zein/SbQ before and after post-treatments, (b) schematic illustration of the dynamic wetting process of nanofibre membranes.

Fig. 6 a displays the representative water absorption curves of zein and zein/SbQ before and after post-treatments. A schematic of the water absorption curve is also shown in Fig. 6 b. The induced weight changes were recorded by the precision electronic balance during the water absorption measurements as well as when the clamp approached and retracted from the

deionized water; the entire process provided a rich source of data on the surface properties and the dynamic wetting behaviour of the samples.

The curve started at point A where the weight was zeroed out. When the sample moved towards the water, the sample weight was still zero until it contacted the water. A negative weight change can be observed when the sample is hydrophobic and vice versa if the sample is hydrophilic. In the case of hydrophobic samples, the surface tension of the water/air interface resists interruption, a factor that contributes to a negative force input from point B to point C. The change between point C and point D is due to the sudden break of the water film when it wicks up around the surface of the sample that was already in the water. After the sample reached its wetting length (5 cm), it was kept static for 30 seconds to adsorb water. Point D to Point E represents the weight increase from water absorption after 30 seconds. As the sample started to retract from point E, the water film formed on both surface sides of the samples that stopped it from retracting, and this adhesive force contributed to an obvious increase in weight. At point F, the water film broke, and the weight assumed a value equal to the quantity of water adsorbed.

According to the analysis above, zein behaves as a hydrophobic substrate because of the negative force curve from 10 ~ 20 seconds. After ~ 20 seconds, the water surface tension is suddenly interrupted and the substrate can absorb water very rapidly and achieve equilibrium within 10 seconds (at 30 seconds, the water absorption curve plateaus). In general, the adhesive force between water and sample surface is not appreciable. However, after the incorporation of SbQ, the surface of the sample is far more hydrophilic as evidenced by the positive force curve in Fig. 6a over the same range as zein. This finding confirmed the speculation that SbQ mainly distributes itself on the surface of the fibre and thus can greatly affect the surface properties. As opposed to the 30 seconds required for zein, zein/SbQ achieved its absorption equilibrium within an order of magnitude less time, i.e., 3 seconds, but showed a very small adhesive force between the sample surface and the water (twice as small as observed for zein). This phenomenon could be partially attributed to the surface bound AcOH in zein, which could form a water-friendly interface. The post-treatments also showed a very significant effect on the dynamic water absorption behaviour. After thermal treatment, the sample became hydrophobic, a finding that might be attributed to the removal of the bound AcOH during the thermal process that forces zein to act as the sole contributor to the surface properties. In addition, the changes in the secondary structure of zein induced by thermal treatment may also lead to increased surface hydrophobicity. Additionally, the UV illumination induced photocrosslinking, a phenomenon that caused SbQ to become much more hydrophobic,^{24, 25} so the sample surface responded in kind. Yet, the dynamic water absorption behaviour was similar to the zein/SbQ nanofibrous membrane, indicative of the presence of AcOH. The Zein/SbQ nanofibrous membrane after a combined post-treatment displayed hydrophobic behaviour, low water absorption rate, and a high adhesive force at the water interface.

Mechanical properties

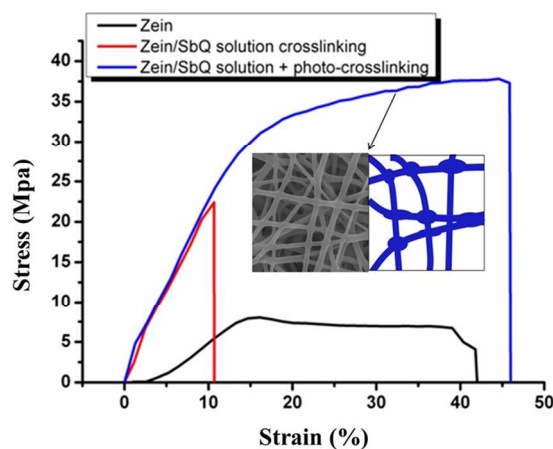


Fig. 7 Stress/strain curves for electrospun zein nanofibrous membranes before and after crosslinking.

The mechanical properties of electrospun zein fabric samples were tested to determine if they were altered by the post-treatments. Samples were cut in a parallel fashion to the take-up roll direction. As shown in the stress/strain curves in Fig. 7, the solution crosslinked zein materials undergo brittle failure as opposed to irregular breakage before failing for the control fabric. Similar results were observed previously with GDA- and formaldehyde-crosslinked zein fabrics, a result that was attributed to improved fiber adhesion.^{14, 18} However, in the case of the two-step crosslinked zein fabrics, they showed very different behaviour during the tensile test. When the applied strength was further increased, the material showed a uniform cross sectional deformation because of the junction points which were present throughout the fiber matrix and the membrane reached its low yield point before reaching its ultimate tensile strength. This two-step crosslinking process increased both the tensile strength (TS) and elongation, facts that might be attributed to the different fibrous structure after photo-induced crosslinking. The membrane showed a different shape: a grid-like structure was adopted after photo-crosslinking that is able to resist the applied force by more evenly distributing the stress. The joint points were very strong and were major contributors to significantly improved mechanical properties.

Conclusions

A novel two-step crosslinking process is introduced for the first time that coupled a facile electrospinning process with atom efficient thermal and photocuring treatments to successfully synthesize crosslinked zein composite nanofibrous membranes. The incorporation of SbQ contributed to a bead-free structure that also increased the average diameter of the zein nanofibers. After the two-step crosslinking, the nanofibrous membrane displayed a grid-like structure, which significantly improved the mechanical properties of the crosslinked zein nanofibrous membrane. The aldehyde of SbQ was associated with zein in AcOH solution; after the electrospinning process, SbQ distributed throughout the as-spun zein fibers. This assessment was confirmed by SEM, FTIR, and water absorption properties. The type of crosslinked zein nanofibrous membranes presented demonstrated very high mechanical properties features that enhance its value for food packaging, scaffolding materials, and numerous bio-product applications.

Experimental Section

Materials

1-Methyl-4-[2-(4-formylphenyl)-ethenyl]-pyridinium-methosulphate (SbQ) was received from Shanghai Guangyi Printing Equipment Technology Co., Ltd (Shanghai, China) and used as is. Zein ($M_w=35,000 \text{ g mol}^{-1}$) was purchased from Sigma-Aldrich (Shanghai, China); acetic acid was received from Sinopharm Chemical Reagent Co., Ltd (Shanghai, China). All materials were used as received without further purification.

Materials preparation

Electrospinning. First, a specific level of zein powder commingled with SbQ (0 wt-%, 10 wt-%, 20 wt-%) was weighed and dissolved in 12 mL acetic acid (25 wt-%) at room temperature after being vigorously stirred for three hours upon which a homogeneous solution was obtained. The viscosity (NDJ-79), conductivity (DDS-11C), and surface tension (QBZY) of the electrospinning solutions were obtained.

The solutions were placed in a syringe with a blunt end stainless steel needle. The applied voltage was 25 kV with a working distance of 15 cm from the stainless steel needle tip to a collector site (circular rotating drum), and the flow rate was maintained at 1 mL/h. The nanofibres were collected on the circular rotating drum that was covered with aluminium foil. The compositional characteristics of the as-spun nanofibrous membranes were demarcated as zein (control), zein90/SbQ10 (90:10 zein:SbQ, wt-%), zein80/SbQ20 (80:20 zein:SbQ, wt-%). **Post treatment.** The electrospun nanofibrous membranes of zein, zein90/SbQ10, and zein80/SbQ20 were thermally treated at 150 °C for 2 hrs, followed by UV illumination for another 4 hrs. The UV light source was XQ500W with 350-500W capacity (Shanghai Lanshen Electric Company Ltd.). To better understand the influence of thermal treatment and UV illumination, control samples with only thermal treatment or UV illumination were also prepared.

Measurements and characterization

Surface morphology. Scanning electron microscopy (SEM, Quanta 200, Holland FEI Company) was used to investigate the surface morphology of the zein and zein/SbQ composite nanofibres before and after treatments. The samples were coated with a thin layer of gold by sputtering before the SEM imaging. Diameters of the electrospun nanofibers were measured by Adobe Acrobat 7.0 professional from SEM images, while 100 fibers were analyzed for each sample to obtain an average fibre diameter.

FTIR analysis. The chemical functional groups in the range of 4000-650 cm^{-1} of zein/SbQ composite nanofibers before and after post-treatment were investigated by Fourier Transform Infrared Spectroscopy (FTIR, Nicolet Nexus, Thermo Electron Corporation) using ATR reflection. The spectra were recorded with 16 scans at a resolution of 4 cm^{-1} .

Thermal properties. The thermal properties of the nanofibres were investigated by differential scanning calorimetry (DSC) (TA-Q2000, TA Instruments Company) and thermal gravimetric analysis (TGA) (TA-Q5000, TA Instruments Company). DSC analyses were carried out with approximately 6 mg of samples under N_2 as a purge gas. Initially, the samples were equilibrated at 25 °C then they were heated to 200 °C at 10 °C/min. TGA was performed from room temperature to 500 °C at a heating rate of 10 °C/min under nitrogen.

Water absorption behaviour. The dynamic wetting behaviour of the samples was tested by a Dynamic Contact Angle Meter and a Tensiometer (DCAT 21, Dataphysics Company). Sample

having a size of 1 cm × 3 cm were prepared. The samples were clamped and immersed into water (see Fig. 7). The weight of the specimen was recorded during the process and the water absorbency process was plotted as a function of time.

Mechanical properties. Mechanical properties of the zein and zein/SbQ composite membranes before and after the treatment were tested using a uniaxial testing machine (INSTRON1185, Instron Company, USA) at a crosshead speed of 10 mm/min and gauge length of 5 cm. The samples were prepared in a strip shape with dimensions of 10 cm (length) × 1 cm (width). The thicknesses of the samples were measured using a DUALSCOPE MPO digital micrometre having a precision of 1 μm , and 10 different points for each specimen were measured to get an average thickness.

Acknowledgements

This research was financially supported by the National High-tech R&D Program of China (2012AA030313), Changjiang Scholars and Innovative Research Team in University (IRT1135), National Natural Science Foundation of China (51006046, 51203064, 21201083 and 51163014). Q.Q.Wang. and A.G.Nandgaonkar. contributed equally in carrying out the experiments, analyzing the results, and writing the manuscript.

Notes and references

- ^aKey Laboratory of Eco-Textiles, Ministry of Education, Jiangnan University, 1800 Lihi Avenue, Wuxi, Jiangsu Province, Wuxi 214122, P.R. China. (E-mail: qfwei@jiangnan.edu.cn).
- ^bState Key Lab of Pulp & Paper Science and Technology of the Ministry of Education, Qilu University of Technology, Jinan, 250353, Shandong, P.R. China. (E-mail: lucian.lucia@gmail.com).
- ^cFiber and Polymer Science Program, North Carolina State University, Raleigh, NC 27695, USA.
- ^dThe Laboratory of Soft Materials & Green Chemistry, Departments of Chemistry, Wood & Paper Science (Forest Biomaterials), North Carolina State University, Raleigh, NC 27695, USA.

- 1 T. Subbiah, G. Bhat, R. Tock, S. Parameswaran and S. Ramkumar, *J Appl Polym Sci*, 2005, **96**, 557-569.
- 2 S. H. Lim and H. Mao, *Adv. Drug Deliv. Rev.*, 2009, **61**, 1084-1096 (DOI:DOI: 10.1016/j.addr.2009.07.011).
- 3 E. Kenawy, F. I. Abdel-Hay, M. H. El-Newehy and G. E. Wnek, *Materials Science and Engineering: A*, 2007, **459**, 390-396 (DOI:DOI: 10.1016/j.msea.2007.01.039).
- 4 J. Chen, G. Chang and J. Chen, *Colloids Surf. Physicochem. Eng. Aspects*, 2008, **313-314**, 183-188 (DOI:DOI: 10.1016/j.colsurfa.2007.04.129).
- 5 P. Gibson, H. Schreuder-Gibson and D. Rivin, *Colloids Surf. Physicochem. Eng. Aspects*, 2001, **187-188**, 469-481 (DOI:DOI: 10.1016/S0927-7757(01)00616-1).
- 6 Y. Wang and L. Chen, *Macromolecular Materials and Engineering*, 2012, **297**, 902-913.
- 7 F. Kayaci and T. Uyar, *Carbohydr. Polym.*, 2012, **90**, 558-568.
- 8 D. Alkan, L. Y. Aydemir, I. Arcan, H. Yavuzdurmaz, H. I. Atabay, C. Ceylan and A. Yemencioğlu, *J. Agric. Food Chem.*, 2011, **59**, 11003-11010.
- 9 K. Shi, J. L. Kokini and Q. Huang, *J. Agric. Food Chem.*, 2009, **57**, 2186-2192.
- 10 Y. P. Neo, S. Ray, J. Jin, M. Gizdavic-Nikolaidis, M. K. Nieuwoudt, D. Liu and S. Y. Quek, *Food Chem.*, 2013, **136**, 1013-1021.
- 11 A. R. Unnithan, G. Gnanasekaran, Y. Sathishkumar, Y. S. Lee and C. S. Kim, *Carbohydr. Polym.*, 2014, **102**, 884-892.
- 12 S. Gong, H. Wang, Q. Sun, S. Xue and J. Wang, *Biomaterials*, 2006, **27**, 3793-3799.
- 13 G. W. Selling, D. J. Sessa and D. E. Palmquist, *Polymer*, 2004, **45**, 4249-4255.
- 14 G. W. Selling, K. K. Woods and A. Biswas, *Polym. Int.*, 2011, **60**, 537-542.
- 15 G. W. Selling, K. K. Woods and A. Biswas, *J Appl Polym Sci*, 2012, **123**, 2651-2661.

Journal Name

- 16 D. J. Sessa, A. Mohamed, J. A. Byars, S. A. Hamaker and G. W. Selling, *J Appl Polym Sci*, 2007, **105**, 2877-2883.
- 17 D. J. Sessa, A. Mohamed and J. A. Byars, *J. Agric. Food Chem.*, 2008, **56**, 7067-7075.
- 18 G. W. Selling, K. K. Woods, D. Sessa and A. Biswas, *Macromolecular Chemistry and Physics*, 2008, **209**, 1003-1011.
- 19 C. Yao, X. Li and T. Song, *J Appl Polym Sci*, 2007, **103**, 380-385.
- 20 Y. Yang, L. Wang and S. Li, *J Appl Polym Sci*, 1996, **59**, 433-441.
- 21 N. Reddy, Y. Li and Y. Yang, *Biotechnol. Prog.*, 2009, **25**, 139-146.
- 22 S. Kim, D. Sessa and J. Lawton, *Industrial crops and products*, 2004, **20**, 291-300.
- 23 E. S. Cockburn, R. S. Davidson and J. E. Pratt, *J. Photochem. Photobiol. A.*, 1996, **94**, 83-88.
- 24 J. Xu, H. Bai, C. Yi, J. Luo, C. Yang, W. Xia and X. Liu, *Carbohydr. Polym.*, 2011, **86**, 678-683.
- 25 Y. Tao, J. Xu, M. Chen, H. Bai and X. Liu, *Carbohydr. Polym.*, 2012, **88**, 118-124.
- 26 Y. P. Neo, S. Ray, A. J. Easteal, M. G. Nikolaidis and S. Y. Quek, *J. Food Eng.*, 2012, **109**, 645-651.
- 27 T. Song and C. Yao, *Chinese Journal of Polymer Science*, 2010, **28**, 171-179.
- 28 K. Peters and F. M. Richards, *Annu. Rev. Biochem.*, 1977, **46**, 523-551.
- 29 V. Cabra, R. Arreguin, A. Galvez, M. Quirasco, R. Vazquez-duhalt and A. Farres, *J. Agric. Food Chem.*, 2005, **53**, 725-729.
- 30 A. Habeeb and R. Hiramoto, *Arch. Biochem. Biophys.*, 1968, **126**, 16-26.